Growth Mechanisms of Copper Nanocrystals on Thin Polypyrrole Films by Electrochemistry

D. K. Sarkar, X. J. Zhou, A. Tannous, and K. T. Leung*

Department of Chemistry, University of Waterloo, Waterloo, Ontario N2L 3G1, Canada

Received: September 9, 2002; In Final Form: January 21, 2003

Copper nanocrystals have been grown on thin polypyrrole films obtained by electropolymerization on a gold electrode from $CuSO_4$ solution electrochemically in both potentiostatic (constant potential) and galvanostatic (constant current) modes. A variety of copper nanostructures including fractals, nanowires, and cubic nanocrystals have been observed in the galvanostatic mode, in contrast to a single predominant type of nanostructures obtained by manipulating the under-peak potential (fractals) or over-peak potential (cubic nanocrystals) in the potentiostatic mode. The homogeneous distribution of nanocrystals observed at over-peak potential is consistent with an instantaneous growth mechanism. Depth profiling by X-ray photoelectron spectroscopy further reveals the presence of an ultrathin copper oxide layer on the surface of these nanocrystals.

The fabrication of assemblies of "perfect" nanometer-scale quantum crystals identically replicated in such a state that they could be manipulated and understood as pure macromolecular substances is an important challenge in modern materials research with significant fundamental and technological implications. The recent interest in these nanomaterials is due to the dependence of optical,[1] magnetic,[2] and electronic properties on the particle size in the nanoscale, which is markedly different from their corresponding bulk properties. The preparation and characterization of these nanomaterials have thus motivated a vast amount of work. In particular, nanoparticles have been grown in physical,[3,4] and electrochemical processes[5−9] with some involving the use of a scanning tunneling microscope (STM) tip.[10] In the physical deposition process, the deposition rate and the surface diffusion coefficient determine the shape, size, and density of the nanomatter on a specific surface.[11] On the other hand, the concentration and pH of the electrolyte, as well as the applied potential, play a prominent role in the electrochemical deposition process.[12] The number of active nucleation sites is proportional to the applied potential on the electrode because the effective nucleation barrier becomes lower with increasing applied potential.[13] Depending on the surface (interface) energies of the substrates and the deposited materials, both progressive and instantaneous growth mechanisms have been observed in the electrochemical deposition process. In the Volmer−Weber growth process, the growth mechanism is instantaneous due to the large difference in the surface energies of the substrate and the deposited materials.[14] For instance, nanoscale quantum wires have been obtained on diblock polymers by utilizing the difference in the surface energies of the two polymers.[15,16]

Deposition of different metal nanostructures on a variety of substrates has been achieved by electrochemistry.[17] As one of the most popular organic semiconductor materials, polypyrrole has been used in a variety of industrial applications, including solid-state diodes [grown by electrochemistry on n-type Si(100)].[18,19] Several recent studies have demonstrated the fractal growth of copper on polypyrrole and the plausible chemical interactions between copper and polypyrrole.[20,21] However, the fabrication of monodispersed nanometer-size copper crystals with precise control of the metric parameters (shape, size, density) on thin polypyrrole films remains a major challenge. Despite the potential of exhibiting novel collective properties, the assembly of nanoscale structures into well-defined two- or three-dimensional spatial arrangements as super-nanostructures is poorly understood. Despite the explosive growth in recent research on nanomaterials, the field of nanostructured materials assembly is very much in its infancy, with much of the basic physics, chemistry, and engineering at the nanometer scale being largely unexplored. In the present work, we investigate the growth mechanism of near-perfect cubic copper nanocrystals on thin polypyrrole film substrates by electrochemistry, with the goal being to develop a general procedure for controlling the fabrication of quantum crystals with well-defined metric parameters.

Polypyrrole thin films were deposited on a gold electrode by electrochemical polymerization at an applied potential of 0.8 V (versus AgCl/Ag standard potential) in a solution of 0.05 M pyrrole and 0.1 M $NaClO_4$. The thickness of the polypyrrole film controlled by the total amount of charge transfer was estimated to be 100 nm. Copper was then deposited electrochemically on the polypyrrole films in a solution of 0.01 M $CuSO_4$ and 0.1 M $NaClO_4$ under different applied potentials from −0.4 to −1.4 V (versus AgCl/Ag standard potential). Cyclic voltammetric measurement for polycrystalline copper substrates revealed that deposition occurs at a peak potential of −0.56 V (versus AgCl/Ag standard potential). We therefore define potentials that are less and more negative than −0.56 V as under-peak potential (UPP) and over-peak potential (OPP), respectively. Approximately five monolayers of copper for an electrode surface area of 0.28 cm^2 were deposited on a 100-nm-thick polypyrrole film grown under different constant potentials (potentiostatic mode). Copper has also been deposited on the polypyrrole film substrate by keeping the current density through the electrode constant at 0.2 mA/cm^2 for different periods of time (galvanostatic mode). A LEO 1530 field-emission scanning electron microscope (SEM) and a VG Scientific ESCALab 250 X-ray photoelectron spectrometer

* To whom correspondence should be addressed. Electronic mailing address: tong@uwaterloo.ca.

10.1021/jp0269524 CCC: $25.00
Published on Web 03/12/2003

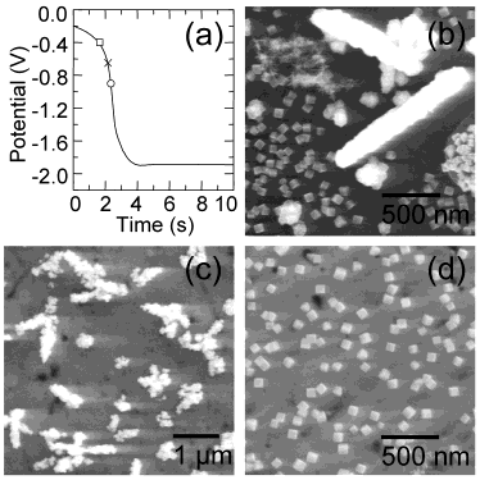

Figure 1. (a) Change in the applied potential (V) as a function of time (s) in the galvanostatic mode for copper deposition on a 100-nm-thick polypyrrole film. The cross at −0.56 V (versus AgCl/Ag standard potential) marks the peak potential for copper deposition obtained from a cyclic voltammetric scan for polycrystalline copper substrate. Potentials that are higher (e.g., open square at −0.4 V) and lower (e.g., open circle at −0.9 V) than −0.56 V are referred to as under-peak potential and over-peak potential, respectively. Panel b shows the corresponding SEM micrograph for copper deposition obtained galvanostatically as shown in panel a, depicting a variety of structures including nanowires, microrods, fractals, and cubic nanocrystals. Panels c and d show SEM micrographs for copper deposition obtained in potentiostatic mode at (c) under-peak potential (−0.4 V) and (d) over-peak potential (−0.9 V), depicting the changes in the predominant nanostructures from fractals to near-perfect cubic nanocrystals.

(XPS) with a monochromatic Al Kα light source have been used to analyze, respectively, the surface morphology and chemical environment of the resulting copper nanostructures deposited on the polypyrrole films.

Figure 1 compares the SEM micrographs of the copper nanostructures deposited on the 100-nm-thick polypyrrole substrates galvanostatically and potentiostatically. In the galvanostatic mode (of copper deposition), the current density passing through the electrodes was kept constant at 0.2 mA/cm^2, during which the potential on the electrode was found to decrease abruptly from near zero to −1.9 V (versus AgCl/Ag standard potential) in less than 4 s in our experiments, as shown in Figure 1a. Similar current−voltage change has also been reported recently for the deposition of soft magnetic materials by electrochemistry.[22] It should be noted that hydrogen evolution occurs at −1.65 V (versus AgCl/Ag standard potential).[23] Because the applied current after 4 s corresponds to the total current for both copper deposition and hydrogen evolution, it is difficult to determine the amount of copper deposited galvanostatically. Evidently, the corresponding SEM micrograph of the resulting nanostructures obtained galvanostatically shown in Figure 1b reveals the presence of a number of remarkably different forms of nanostructures, including cubic nanocrystals (∼80 nm side length) individually or clustering together, nanowires, and microrods or clusters. Closer examination of an individual rod shows that it consists of near-perfect cubic copper nanocrystals. These copper structures deposited galvanostatically are markedly different from those obtained potentiostatically in both UPP and OPP regimes. In particular, Figure 1c shows that copper nanostructures deposited at −0.4 V (versus AgCl/Ag standard potential) in the UPP region correspond to fractal-like or dendrite structures, which are consistent with the UPP deposition made by Liu et al.[21] In contrast, uniformly dispersed near-perfect cubic nanocrystals

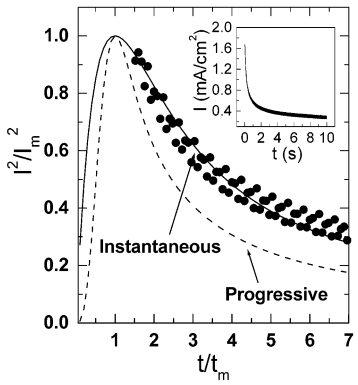

Figure 2. Comparison of square of the normalized current density (I/I_m) as a function of the normalized time (t/t_m) for experimental results for copper deposition on a 100-nm-thick polypyrrole film potentiostatically at −0.9 V over-peak potential (●) with calculated data for instantaneous nucleation (—) prescribed by eq 1 and for progressive nucleation (− − −) described by eq 2. The "raw" experimental current density (I) as a function of time (t) is shown in the inset.

(of ∼80 nm side length) are observed for copper deposition at −0.9 V (versus AgCl/Ag standard potential) in the OPP region, as illustrated in Figure 1d.

The normalized current density for instantaneous nucleation followed by diffusion-limited growth generally follows the relation

$$\frac{I^2}{I_m^2} = \frac{1.9542}{t/t_m}\{1 - \exp[-1.2564(t/t_m)]\}^2 \qquad (1)$$

while that for progressive nucleation observes the equation

$$\frac{I^2}{I_m^2} = \frac{1.2254}{t/t_m}\{1 - \exp[-2.3367(t/t_m)^2]\}^2 \qquad (2)$$

where t_m corresponds to the time when the maximum current density I_m is reached. For example, Ji et al. have used the above equations to explain the growth of copper on Si substrates.[5] Figure 2 shows the square of the normalized current density (I/I_m) as a function of the normalized time (t/t_m) while the insert depicts the time evolution of the current density for copper deposition on thin polypyrrole films at a constant applied potential of −0.9 V (versus AgCl/Ag standard potential). The solid line represents the instantaneous growth mode (eq 1), while the dashed line shows the progressive growth mode (eq 2). Evidently, the experimental data is found to be in excellent agreement with the instantaneous growth curve, in marked contrast to the progressive growth curve. The instantaneous growth mode can also be inferred from the corresponding SEM micrograph in Figure 1d, which shows copper nanocrystals of well-defined size and shape. In the instantaneous growth mode, the incoming copper atoms are expected to occupy all of the available nucleation sites on the substrate simultaneously at the very early instant of the start of the deposition process. Once all of the nucleation sites are occupied, further increase in the deposition time would only increase the size of the nanocrystals and not their number density because no new nucleation sites are created. In contrast, nucleation sites are created throughout the deposition period in the case of progressive nucleation growth, resulting in a wide range of nanocrystal sizes at different stages of the growth process upon creation.[5] The narrow size distribution of the nanocrystals, as depicted in Figure 1d, therefore supports the instantaneous growth mode.

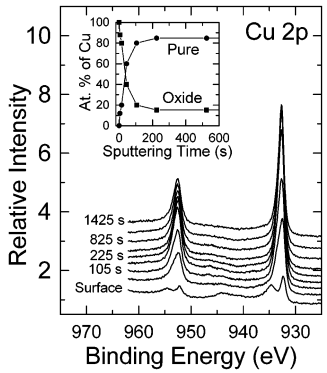

Figure 3. Depth profiles of Cu 2p photolines of the copper nanocrystals deposited potentiostatically at −0.9 V over-peak potential on a 100-nm-thick polypyrrole film. Inset shows the relative atomic percentages of copper in oxide and pure forms as a function of the sputtering time.

Instantaneous nucleation commonly occurs when the surface energy of the substrate is considerably different from that of the deposited material. For example, the growth mode is instantaneous in the case of Cd deposition on Si(111) because of the large difference in the surface energy between Cd and silicon.[24] In accord with any metal−polymer system, the surface energy difference of which is much higher[25] compared to that for the metal−silicon system, the deposition of copper on polypyrrole thin films follows the instantaneous growth mechanism and a homogeneous distribution of copper nanoparticles (with well-defined size and shape) is observed.

To access the quality of the nanocrystals obtained electrochemically, the chemical composition of these copper nanocrystals is examined using XPS as a function of depth (depth profiling). Figure 3 shows the corresponding depth profiles of Cu 2p photopeaks for copper nanocrystals deposited on a 100-nm-thick polypyrrole film obtained potentiostatically at −0.9 V (versus AgCl/Ag standard potential) shown in Figure 1d. In addition to the main photoline for Cu $2p_{3/2}$ ($2p_{1/2}$) of atomic Cu at 932.5 eV (952.3 eV), a higher-lying Cu $2p_{3/2}$ ($2p_{1/2}$) feature at 934.7 eV (954.7 eV) with fwhm of 4.3 eV and a weak satellite peak near 944 eV confirm the presence of CuO.[26] Furthermore, despite the very similar binding energies of the Cu $2p_{3/2}$ photopeaks for both Cu (∼932.6 eV) and Cu_2O (∼932.5 eV) (due to the completeness of $3d^{10}$ electrons in their electronic structures),[27] the LMM Auger line for Cu_2O at 916.6 eV kinetic energy is sufficiently well resolved from the corresponding Auger line of Cu at 918.6 eV kinetic energy that it can indeed be used to confirm the presence of Cu_2O on the surface of the nanocrystals. The inset of Figure 3 shows the relative atomic percentages of Cu for the surface CuO/Cu_2O and pure copper in the nanocrystals as a function of the sputtering time. The ratio of the LMM Auger peak intensities has been used to calculate the relative amounts of Cu_2O and Cu in the photoline at 932.5 eV. Evidently, the observed features attributable to CuO/Cu_2O are found to greatly reduce to its minimal level (∼20%) after sputtering for 100 s. The observed changes in the oxide (CuO/Cu_2O) percentage are consistent with the presence of a thin oxide layer due to the oxidization of copper nanostructures in air and not in the solution (in the latter case the oxide would be expected to be more evenly distributed inside the nanocrystals). From consideration of the intensity of the photolines (which is proportional to the volume of the photoelectron emitter material), we estimate that the oxide shell encasing a ∼80 nm copper nanocrystal is 3 nm thick.

In summary, we have investigated the growth mechanism of copper nanocrystals electrochemically deposited on a 100-nm-thick polypyrrole film in galvanostatic and potentiostatic modes. In the galvanostatic mode, a variety of nanostructures including nanowires, microwires, and fractals, as well as cubic nanocrystals, have been observed. In contrast, only fractal-like growth is found in the UPP region, while near-perfect cubic copper nanocrystals with a narrow size distribution are observed in the OPP region in the potentiostatic mode. The copper growth mode is found to follow the Volmer−Weber (i.e., instantaneous) nucleation mechanism, which is consistent with the large surface energy difference between copper and the conducting polymer (polypyrrole) substrate. Finally, we have also found evidence of an ultrathin layer of copper oxides (estimated to be less than 3 nm thick) on the surfaces of the copper nanocrystals, which is believed to be the result of air oxidation.

Acknowledgment. This work was supported by the Natural Sciences and Engineering Research Council of Canada.

References and Notes

(1) Wang, Z.; Chan, C. T.; Zhang, W.; Ming, N.; Sheng, P. *Phys. Rev. B* **2001**, *64*, 113108.
(2) Bubendorff, J. L.; Beaurepaire, E.; Meny, C.; Bucher, J. P. *J. Appl. Phys.* **1998**, *83*, 7043.
(3) Cole, D. H.; Shull, K. R.; Rehn, L. E.; Baldo, P. *Phys. Rev. Lett.* **1997**, *78*, 5006.
(4) Fischer, B.; Brune, H.; Barth, J. V.; Fricke, A.; Kern, K. *Phys. Rev. Lett.* **1999**, *82*, 1732.
(5) Ji, C.; Oskam, G.; Searson, P. C. *Surf. Sci.* **2001**, *492*, 115.
(6) Schuster, R.; Kirchner, V.; Xia, X. H.; Bittner, A. M.; Grtl, G. *Phys. Rev. Lett.* **1998**, *80*, 5599.
(7) Morin, S.; Lachenwitzer, A.; Magnussen, O. M.; Behm, R. J. *Phys. Rev. Lett.* **1999**, *83*, 5066.
(8) Sieradzki, K.; Brankovic, S. R.; Dimitrov, N. *Science* **1999**, *284*, 138.
(9) Strbac, S.; Magnussen, O. M.; Behm, R. J. *Phys. Rev. Lett.* **1999**, *83*, 3246.
(10) Kolb, D. M.; Ullmann, R.; Will, T. *Science* **1997**, *275*, 1097.
(11) Brune, H. *Surf. Sci. Rep.* **1998**, *31*, 121.
(12) Natter, H.; Hempelmann, R. *J. Phys. Chem.* **1996**, *100*, 19525.
(13) Scharifker, B.; Hills, G. *Electrochim. Acta* **1983**, *28*, 879.
(14) Krumm, R.; Guel, B.; Schmitz, C.; Staikov, G. *Electrochim. Acta* **2000**, *45*, 3255.
(15) Lopes, W. L.; Jaeger, H. M. *Nature* **2001**, *414*, 735.
(16) Higgins, A. M.; Jones, R. A. L. *Nature* **2000**, *404*, 476.
(17) Strbac, S.; Magnussen, O. M.; Behm, R. J. *Phys. Rev. Lett.* **1999**, *83*, 3246.
(18) Vermeir, I. E.; Kim, N. Y.; Laibinis, P. E. *Appl. Phys. Lett.* **1999**, *74*, 3860.
(19) Lonergan, M. C. *Science* **1997**, *278*, 2103.
(20) Cioffi, N.; Torsi, L.; Losito, I.; Franco, C. D.; Bari, I. D.; Chiavarone, L.; Scamarcio, G.; Tsakova, V.; Sabbatini, L.; Zambonin, P. G. *J. Mater. Chem.* **2001**, *11*, 1434.
(21) Liu, Y. C.; Yang, K. H.; Ger, M. D. *Synth. Met.* **2002**, *126*, 337.
(22) Azzaroni, O.; Schilardi, P. L.; Salvarezza, R. C. *Appl. Phys. Lett.* **2002**, *80*, 1061.
(23) Oskam, G.; Searson, P. C. *J. Electrochem. Soc.* **2000**, *147*, 2199.
(24) Krumm, R.; Guel, B.; Schmitz, C.; Staikov, G. *Electrochim. Acta* **2001**, *45*, 3255.
(25) Cole, D. H.; Shull, K. R.; Rehn, L. E.; Baldo, P. *Phys. Rev. Lett.* **1997**, *78*, 5006.
(26) Balamurugan, B.; Mehta, B. R.; Shivaprasad, S. M. *Appl. Phys. Lett.* **2001**, *79*, 31276.
(27) Moulder, J. F.; Stickle, W. F.; Sobol, P. E.; Bomben, K. D. *Handbook of X-ray Photoelectron Spectroscopy*; Perkin-Elmer Corp.: Eden Prairie, MN, 1992.